Plant Physiol. (1990) 93, 1303–1311
0032-0889/93/90/1303/09/$01.00/0

Received for publication December 11, 1989
Accepted March 15, 1990

Regulation of Phosphoenolpyruvate Carboxylase from the Green Alga *Selenastrum minutum*[1]

Properties Associated with Replenishment of Tricarboxylic Acid Cycle Intermediates during Ammonium Assimilation

Kathryn A. Schuller, William C. Plaxton, and David H. Turpin*

Department of Biology, Queen's University, Kingston, Ontario, Canada K7L 3N6

ABSTRACT

Two isoforms of phosphoenolpyruvate carboxylase (PEPC) with very different regulatory properties were partially purified from the green alga *Selenastrum minutum*. They were designated $PEPC_1$ and $PEPC_2$. $PEPC_1$ showed sigmoidal kinetics with respect to phosphoenolpyruvate (PEP) whereas $PEPC_2$ exhibited a typical Michaelis-Menten response. The $S_{0.5}$(PEP) of $PEPC_1$ was 2.23 millimolar. This was fourfold greater than the $S_{0.5}$(PEP) of $PEPC_2$, which was 0.57 millimolar. $PEPC_1$ was activated more than fourfold by 2.0 millimolar glutamine and sixfold by 2.0 millimolar dihydroxyacetone phosphate (DHAP) at a subsaturating PEP concentration of 0.625 millimolar. In contrast, $PEPC_2$ showed only 8% and 52% activation by glutamine and DHAP, respectively. The effects of glutamine and DHAP were additive. $PEPC_1$ was more sensitive to inhibition by glutamate, 2-oxoglutarate, and aspartate than $PEPC_2$. Both isoforms were equally inhibited by malate. All of these metabolites affected only the $S_{0.5}$(PEP) not the V_{max}. The regulatory properties of *S. minutum* PEPC *in vitro* are discussed in terms of (a) increased rates of dark carbon fixation (shown to be catalyzed predominantly by PEPC) and (b) changes in metabolite levels *in vivo* during enhanced NH_4^+ assimilation. Finally, a model is proposed for the regulation of PEPC *in vivo* in relation to its role in replenishing tricarboxylic acid cycle intermediates consumed in NH_4^+ assimilation.

It has been proposed the PEPC[2] in C_3 plants functions to replenish TCA cycle intermediates consumed in amino acid biosynthesis (5, 12, 16). During NH_4^+ assimilation, the net synthesis of glutamine and glutamate utilizes 2-oxoglutarate in the GS/GOGAT reactions (17). Increased rates of NH_4^+ assimilation have been correlated with elevated rates of dark carbon fixation in cyanobacteria, green algae, and higher plants (4–6, 10, 11, 21, 22, 24) and these elevated rates of dark carbon fixation have been attributed to increased activity of PEPC. However, the factors responsible for increased PEPC activity have not been identified.

In contrast to the situation in C_3 plants, the regulation of PEPC in C_4 and CAM plants is well understood (23). The enzyme purified from leaf tissue of C_4 and CAM plants is inhibited by malate and activated by glucose-6-P (1). In the CAM plant *Crassula argentea*, PEPC undergoes interconversion between a more active tetrameric 'night form' (less sensitive to malate inhibition, more sensitive to glucose-6-P activation) and a less active dimeric 'day form' (more sensitive to malate inhibition, less sensitive to glucose-6-P activation) (35, 36). Both CAM and C_4 PEPC are regulated in a light dependent manner by protein phosphorylation (8, 20). The phosphorylated enzyme, which is more abundant in the dark in CAM plants and in the light in C_4 plants, is less sensitive to malate inhibition than the dephosphorylated enzyme. In the C_4 plant maize, where the day form of PEPC is more active than the night form, phosphorylation status is the most important factor, and changes in oligomeric state apparently are not involved in regulation by light (15). The properties of C_4 and CAM PEPC are consistent with its role in the C_4 acid cycle of photosynthesis. PEPC from C_3 plants and nonphotosynthetic forms of the enzyme from C_4 and CAM plants might, therefore, be expected to have very different properteis from the photosynthetic forms of PEPC (1, 12). PEPC from C_3 plants has a lower K_m (PEP) and is less sensitive to malate inhibition and glucose-6-P activation than the C_4 enzyme (12). Beyond this, very little is known of the regulation of PEPC in C_3 plants, especially as pertains to its potential anaplerotic functioning during NH_4^+ assimilation.

In the present study we confirm the stimulation of dark carbon fixation associated with an increase in the rate of NH_4^+ assimilation in a C_3 plant, the green alga *Selenastrum minutum*, and present evidence that PEPC is the predominant enzyme catalyzing this process. We also report the partial purification of two isoforms of PEPC from *S. minutum* and examine their regulatory properties. This allows us to propose an integrative model for the regulation of PEPC in a C_3 plant during increased demand for the replenishment of TCA cycle intermediates consumed in the assimilation of NH_4^+ into amino acids.

[1] Supported by the Natural Sciences and Engineering Research Council of Canada.

[2] Abbreviations: PEPC, phosphoenolpyruvate carboxylase; DHAP, dihydroxyacetone phosphate; DIC, dissolved inorganic carbon; FPLC, fast protein liquid chromatography; GOGAT, glutamine oxoglutarate aminotransferase; GS, glutamine synthetase; n_H, Hill coefficient; PEP, phosphoenolpyruvate; PK, pyruvate kinase; PK_c, cytosolic pyruvate kinase; Rubisco, ribulose bisphosphate carboxylase/oxygenase.

MATERIALS AND METHODS

Materials

The green alga *Selenastrum minutum* (Naeg.) Collins (UTEX 2459) was cultured in NO_3^--limited chemostats as previously described (4). The medium was buffered to pH 8.0 with 25 mM Hepes-KOH. The steady state growth rate of cells for dark carbon fixation and metabolite experiments was 0.3 d^{-1} and for enzyme extraction and purification it was 1.2 d^{-1}. All biochemicals and malate dehydrogenase were from Sigma Chemical Co. Other coupling enzymes were from Boehringer-Mannheim. $Na_2{}^{14}CO_3$ was from Nordion International Inc. All other reagents were analytical grade.

Spectrophotometric PEPC Assay

The PEPC reaction was coupled with the malate dehydrogenase reaction and assayed at 25°C by monitoring NADH utilization at 340 nm using a Varian DMS 200 spectrophotometer. The standard assay contained 25 mM Bis Tris Propane (pH 8), 15% (v/v) glycerol, 5 mM $MgCl_2$, 5 mM $KHCO_3$, 5 mM DTT, 0.2 mM NADH, 2.5 mM PEP, and 10 units malate dehydrogenase in a final volume of 1 mL. Assays were initiated by addition of PEPC. One unit is defined as the amount of enzyme catalyzing the utilization of 1 μmol $NADH \cdot min^{-1}$.

Dark Carbon Fixation and Metabolite Analyses

Dark carbon fixation was assayed by following the incorporation of $H^{14}CO_3^-$ into acid stable products in the dark as previously described (34), except that unfixed counts were removed by drying the sample in a stream of air and redissolving in 1 mL of kill solution, three times. The dried sample was taken up in 1 mL H_2O and 2 mL Aquasol II (Dupont) liquid scinitillation cocktail. Experimental protocols for the extraction in $CHCl_3$-methanol and the analysis of metabolites were as previously described (30, 32).

Radiometric PEPC and PEP Carboxykinase Assay

S. minutum cells growing in a chemostate at a rate of 0.3 d^{-1} or in batch culture (13) were extracted in the medium of Jiao and Chollet (8) with 30 mM NaF added and only 10% (v/v) glycerol. The homogenate obtained after two passes through a French press at 18,000 p.s.i. was used in the assay. The assay buffer contained, in a final volume of 1 mL, 50 mM Hepes-KOH (pH 8), 10 mM $MgCl_2$, 5 mM DTT, 1 mM NADH, 5 units malate dehydrogenase, 5 mM PEP, 0.5 mM ADP (PEP carboxykinase only), and 2 mM $NaHCO_3$ (specific radioactivity, 4.5 μCi/μmol DIC). The assay was initiated with the addition of extract and run in the dark. Incorporation of ^{14}C into acid stable products was determined as above. PEPC activity was taken as the rate in the absence of ADP, and PEP carboxykinase activity was calculated as the difference between this rate and that obtained in the presence of ADP.

Pyruvate Carboxylase and NAD-Malic Enzyme Assays

Crude cell extracts were prepared as described for the radiometric PEPC and PEP carboxykinase assay (see above) except that the extraction buffer contained 100 mM Hepes-KOH (pH 7.8), 2 mM EDTA, and 10 mM DTT. The assay buffer contained, in a final volume of 1 mL, 100 mM Hepes-KOH (pH 7.8), 10 mM $MgSO_4$, 5 mM DTT, 1 mM NADH, 10 units malate dehydrogenase, 4 mM ATP, 0.15 mM acetyl CoA, 10 mM pyruvate, and 10 mM $KHCO_3$ (specific radioactivity, 8.56 μCi/μmol DIC). The assay was initiated with the addition of extract and run in the dark. Incorporation of label into acid stable products was determined as above. For malic enzyme, the assay procedure was the same as for pyruvate carboxylase, except that the pH was 7.0 and ATP was omitted.

Buffers Used in PEPC Purification

Buffer A: 25 mM K-Pi (pH 7.0), 20% (v/v) glycerol, 5 mM malate, 2 mM DTT, 1 mM EDTA, 10 mM $MgCl_2$, 0.1% (v/v) Triton X-100, 4% (w/v) PEG-8000, and 2 mM PMSF. Buffer B: 10 mM K-Pi (pH 7.5), 20% (v/v) glycerol, 5 mM malate, 2 mM DTT, 1 mM EDTA, and 5 mM $MgCl_2$. Buffer C: As for buffer B but with 1 M KCl added. Buffer D: 25 mM KPi (pH 7.0), 20% (v/v) glycerol, 5 mM malate, 5 mM thiourea, 2 mM DTT, 1 mM EGTA, 1 mM EDTA, 10 mM $MgCl_2$, 1 mM NaF, 1 mM PMSF, 50 mM KCl, and 0.02% (w/v) NaN_3.

Native Molecular Mass Determination

Native molecular mass estimations were made using a 100 mL FPLC Superose 6 HR 16/50 column equilibrated with buffer D. The sample, 200 to 300 mg protein in a volume of 2 mL, was applied to the column at a flow rate of 0.3 mL/min. Molecular masses were determined from a plot of K_{av} (partition coefficient) *versus* log molecular mass for standard proteins: thyroglobulin (669 kD), ferritin (440 kD), and catalase (232 kD). Blue dextran was used to determine the void volume.

Protein Assay

Protein was determined according to the method of Bradford (2) using bovine γ-globulin as standard.

Enzyme Kinetic Analyses

All kinetic studies were performed using the spectrophotometric assay. Apparent $S_{0.5}$ values and Hill coefficients were calculated from Hill plots using Enzfitter (Sigma Chemical Co.), a nonlinear regression program. Activation constants (K_a) were determined using double-reciprocal plots of $1/(v - v_o)$ *versus* 1/[activator]. I_{50} values (inhibitor concentration producing 50% inhibition of enzyme activity) were determined by the method of Job *et al.* (9). All data are the means of duplicate determinations performed on one representative enzyme preparation.

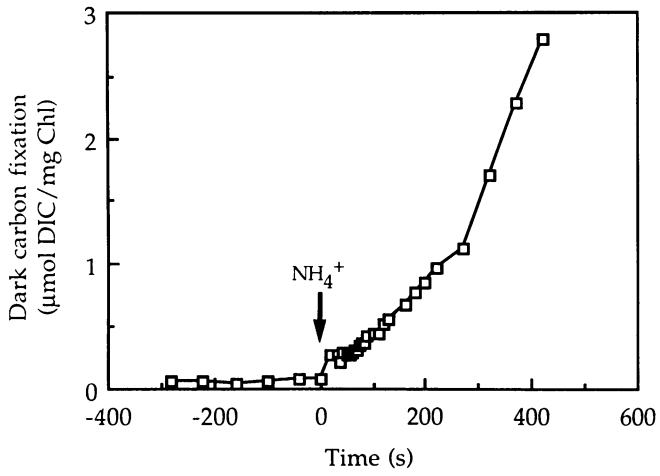

Figure 1. Effect of NH_4^+ assimilation on dark carbon fixation by N-limited *S. minutum*. Cells, at a density of 2 μg Chl/mL, were supplied with $Na_2{}^{14}CO_3$ (specific radioactivity = 6.1 μCi/μmol DIC). Total DIC was 4.3 mM. NH_4Cl (2 mM) was added at time zero. Data are the means of three replicate experiments with different batches of cells.

RESULTS

In Vivo Effects of NH_4^+ Assimilation

Effects of NH4+ Assimilation on Dark Carbon Fixation

Figure 1 shows the effects of resupplying NH_4^+ to N-limited *Selenastrum minutum* cells on incorporation of $H^{14}CO_3^-$ into acid stable products in the dark. Prior to NH_4^+ resupply the rate of dark carbon fixation was low, less than 1 μmol·mg^{-1} Chl·h^{-1}. Immediately following NH_4^+ addition it increased to 12 μmol·mg^{-1} Chl·h^{-1} (0–180 s). Subsequently it increased still further to 40 μmol·mg^{-1} Chl·h^{-1} (270–420 s). PEPC activity in crude cell extracts of *S. minutum* was 30 μmol·mg^{-1} Chl·h^{-1} (radiometric assay) which was almost sufficient to account for the maximum rate of dark carbon fixation. Three other enzymes (PEP carboxykinase, pyruvate carboxylase, and NAD-malic enzyme) which could potentially catalyze dark carbon fixation showed no activity in the carboxylating direction in *S. minutum* extracts (data not shown).

Effects of NH_4^+ Assimilation on PEP and Malate Levels

Resupply of NH_4^+ to N-limited *S. minutum* cells caused a rapid decline in the PEP level (Fig. 2A). Within 5 s of NH_4^+ addition, PEP declined to 41% of its control value. Malate remained relatively constant for the first 2 min of NH_4^+ assimilation (Fig. 2A) but had declined slightly by 5 min. These changes resulted in a large increase in the malate/PEP ratio (Fig. 2B).

Partial Purification of Two Isoforms of PEPC

Two isoforms of PEPC were partially purified from *S. minutum* using the following procedure. All steps were performed at 4°C and PEPC activity was determined using the spectrophotometric assay.

Preparation of the Crude Extract

Cells (50 g) stored at −80°C were thawed into 100 mL of buffer A and passed twice through a French press at 18,000 p.s.i. The homogenate was centrifuged at 24,000*g* for 20 min. The supernatant fluid was retained and designated the crude extract. Inclusion of PMSF, a serine protease inhibitor, in the extraction buffer was very important for the stability of PEPC. Activity losses in the range 40 to 60% occurred between preparation of the crude extract and resuspension of the PEG pellets if PMSF was omitted (data not shown).

PEG Fractionation

The crude extract was brought to 20% (w/v) PEG with a 50% (w/v) solution of PEG-8000 containing 50 mM KH_2PO_4 (pH 7) and 2 mM EDTA. After 20 min stirring, the extract was centrifuged as above and the pellets retained. No PEPC activity was detected in the supernatant fluid.

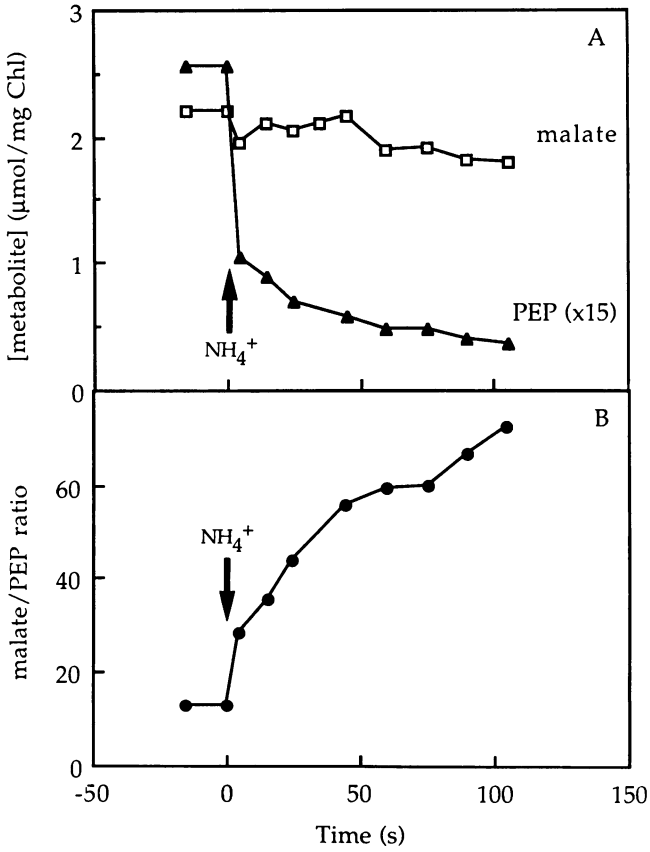

Figure 2. Effect of NH_4^+ assimilation on total cellular malate and PEP levels in N-limited *S. minutum*. NH_4Cl (5 mM) was added at time zero. Data are the means of triplicate analyses of duplicate experiments.

Table I. *Partial Purification of S. minutum $PEPC_1$ and $PEPC_2$*

The standard spectrophotometric assay was used for PEPC activity.

Fraction	Volume	Total Activity	Total Protein	Specific Activity	Yield	Purification
	mL	*units*	*mg*	*units/mg*	%	*-fold*
I. Crude extract	83	63	2573	0.025	100	1.0
II. PEG-8000 fractionation (4–20% w/v)	200	63	1840	0.035	100	1.4
III. Q-Sepharose						
$PEPC_1$	2.3	7.6	209	0.036	12	1.4
$PEPC_2$	5.1	22.4	163	0.138	36	5.5

Q-Sepharose Chromatography

The PEG pellets were resuspended in buffer B to give a protein concentration of 9.2 $mg \cdot mL^{-1}$. Complete recovery of the total PEPC activity assayed in the crude extract was obtained (Table I). The resuspended pellets were centrifuged as above to remove insoluble material and the supernatant liquid was adsorbed batchwise with gentle stirring for 2 h onto 70 mL of Q-Sepharose resin preequilibrated with buffer B. The slurry was then packed into a 2.5-cm diameter column and washed, at 2 mL/min, until the A_{280} fell below 0.05. PEPC activity eluted as two distinct peaks when a 350 mL linear gradient of 0 to 400 mM KCl in buffer B was applied to the column, using an FPLC system (Fig. 3). The early and later eluting peaks were designated $PEPC_1$ and $PEPC_2$, respectively. $PEPC_1$ began to elute at a conductivity of 0.7 mmho which was only marginally above the conductivity of the start buffer (buffer B = 0.4 mmho). $PEPC_2$ was well separated from $PEPC_1$, beginning to elute at 2.0 mmho. The recovery of the total activity-units loaded onto the Q-Sepharose column was 48%, with 25% and 75% of this accounted for in $PEPC_1$ and $PEPC_2$, respectively (Table I). Pooled peak fractions containing $PEPC_1$ or $PEPC_2$ were concentrated approximately 25-fold using an Amicon YM-30 ultrafilter, divided into 200 μL aliquots, frozen with liquid N_2, and stored at −80°C. The purified enzymes were stable for at least 1 month when stored frozen. All subsequent kinetic analyses were performed on the two isoforms of PEPC purified through the Q-Sepharose step.

Kinetic Characterization of the Two Isoforms of PEPC

Effect of pH

The effect of pH on the two isoforms of PEPC was determined in the presence of the substrate and cofactor concentrations used in the standard spectrophotometric assay. As will be shown later (see Table II), the PEP concentration (2.5 mM) was only about 10% above the $S_{0.5}$ for $PEPC_1$ but saturating for $PEPC_2$. Under these conditions, the pH profiles of the two isoforms were very similar with broad optima centered around pH 9.0 (data not shown). Near maximal activity was observed for both between pH 8.0 and 9.5, with a marked drop-off below pH 7.5.

PEP Kinetics

PEP saturation curves suggested a sigmoidal response for $PEPC_1$ (Fig. 4) but hyperbolic for $PEPC_2$ (Fig. 5). Hill plot analyses confirmed the existence of cooperativity in the binding of PEP to $PEPC_1$ (n_H = 1.55) but not to $PEPC_2$ (n_H = 0.81) (Table II). The $S_{0.5}$(PEP) of $PEPC_1$ was 2.23 mM (Table II). This was fourfold greater than the $S_{0.5}$(PEP) of $PEPC_2$ which was 0.57 mM. It should be noted that all PEPC activities reported here were determined in the presence of 15% (v/v) glycerol (see "Materials and Methods"). This was because preliminary studies had shown that glycerol substantially reduced the $S_{0.5}$(PEP) of both isoforms (data not shown). Other authors have cited stabilization of the quaternary structure of

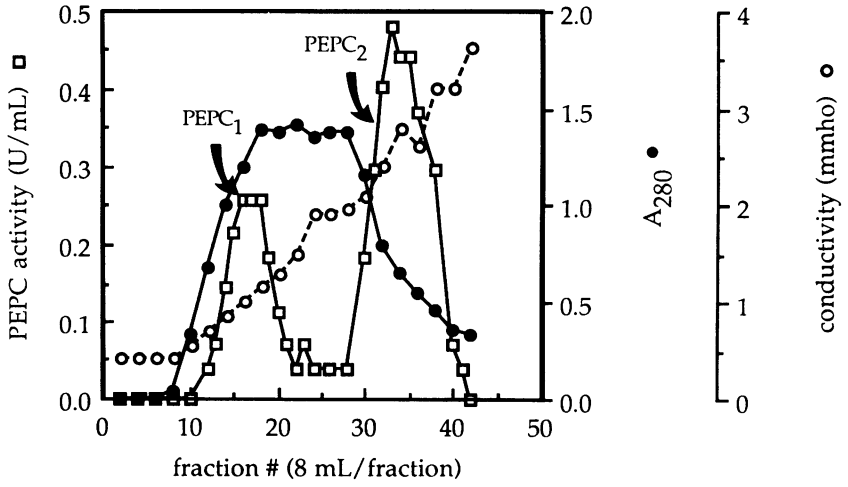

Figure 3. Q-Sepharose chromatography of the 4–20% (w/v) PEG-8000 fraction prepared from a crude extract of *S. minutum*. Details of the procedure are described in the text.

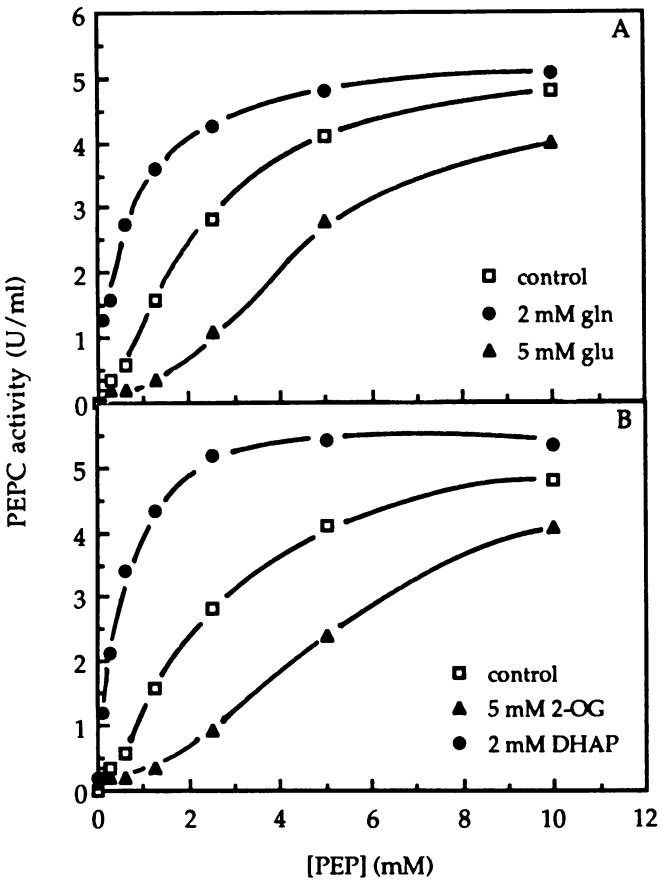

Figure 4. Metabolite effects on PEP saturation kinetics of $PEPC_1$. The standard spectrophotometric assay was used except that the PEP concentration was varied and the effectors were added at the concentrations shown in the figure.

PEPC, due to exclusion of solvent molecules, as the explanation for the favorable effect of glycerol on the affinity of PEPC for its substrate (28, 29, 31).

Metabolite Effects

A variety of metabolites were tested for effects on $PEPC_1$ and $PEPC_2$ at substrating concentrations of PEP (2.5 mM for $PEPC_1$ and 0.32 mM for $PEPC_2$).The following had no effect (±10% of control velocity) on either isoform: glucose-6-P (1 mM), fructose-6-P (1 mM), fructose-1,6-bisP (1 mM), fructose-2,6-bisP (1 mM), acetyl CoA (0.1 mM), Pi (1 mM), and pyruvate (0.4 mM).

Activators

Glutamine markedly activated $PEPC_1$ but hardly affected $PEPC_2$ (Table II; Figs. 4A, 5A). At a concentration of 2 mM, glutamine caused a threefold improvement in the affinity of $PEPC_1$ for PEP (Table II). The K_a(glutamine) of $PEPC_1$ was 0.2 mM (Table III). DHAP activated both forms of PEPC, but $PEPC_1$ more than $PEPC_2$ (Table II; Figs. 4B, 5B). At a concentration of 2 mM, DHAP caused an almost fivefold improvement in the affinity of $PEPC_1$ for PEP but the change was only threefold for $PEPC_2$ (Table II). The K_a(DHAP) of $PEPC_1$ was 1.6 mM. Both activators had their effect on $PEPC_1$ by reducing the sigmoidicity of the PEP saturation curve (Fig. 4, A and B). Neither activator affected V_{max} (Table II).

Inhibitors

Both isoforms of PEPC were inhibited by glutamate, aspartate, 2-oxoglutarate, and malate (Tables II, III; Figs. 4, 5). $PEPC_1$ was more sensitive than $PEPC_2$ to inhibition by glutamate, asparate, and 2-oxoglutarate, but malate inhibited both forms to a similar extent (Table III). The I_{50}(glutamate) of $PEPC_2$ was threefold greater than that of $PEPC_1$, the I_{50}(aspartate) was almost sevenfold greater, and the I_{50}(2-oxoglutarate) was twofold greater (Table III). The two isoforms had similar I_{50} values for malate. The sigmoidicity of the PEP saturation curve for $PEPC_1$ was greatly enhanced by either glutamate (Fig. 4A) or 2-oxoglutarate (Fig. 4B). All four inhibitors caused marked increases in n_H and/or $S_{0.5}$(PEP) for

Table II. *Metabolite Effects on n_H, $S_{0.5}$(PEP) and V_{max} of $PEPC_1$ and $PEPC_2$*

The standard spectrophotometric assay was used except that the PEP concentration was varied and effectors were added at the concentrations shown in the table.

Effector	$PEPC_1$			$PEPC_2$		
	n_H	$S_{0.5}$(PEP)	V_{max}	n_H	$S_{0.5}$(PEP)	V_{max}
		mM	units/mL		mM	units/mL
Control	1.55	2.23	5.29	0.81	0.57	5.71
2 mM glutamine	1.31	0.79	5.84	1.10	0.32	5.15
5 mM glutamate	2.10	4.26	4.62	0.83	0.75	4.78
2 mM malate	1.56	3.98	5.55	0.85	1.09	5.25
2 mM aspartate	1.70	4.03	5.73	0.96	0.65	5.32
5 mM 2-OG	1.76	6.11	5.80	0.76	1.68	6.08
2 mM DHAP	1.42	0.47	5.56	1.10	0.21[a]	6.10[a]

[a] Only 1 determination.

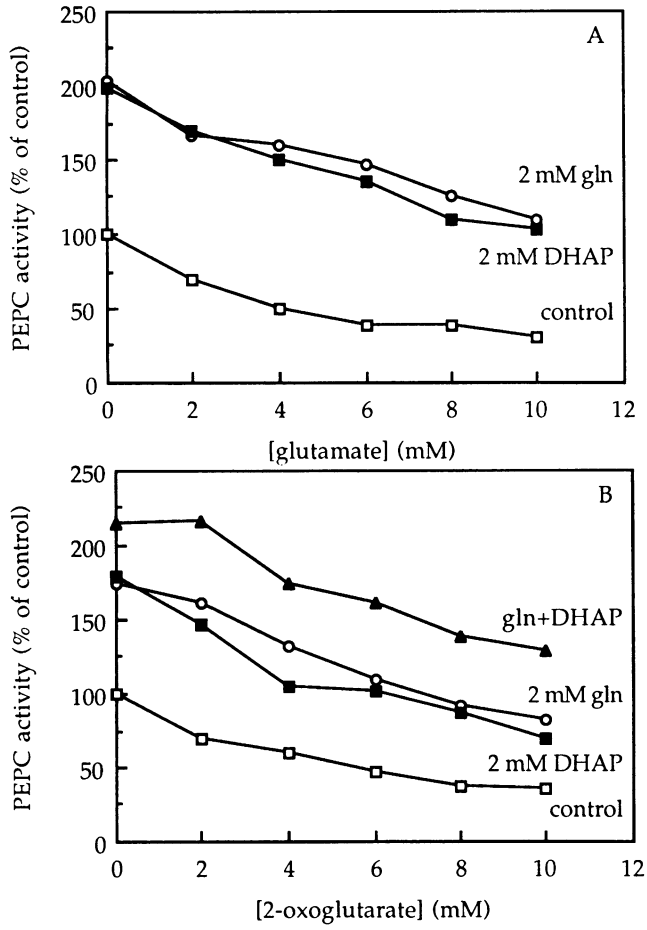

Figure 5. Metabolite effects on PEP saturation kinetics of $PEPC_2$. The standard spectrophotometric assay was used except that the PEP concentration was varied and the effectors were added at the concentrations shown in the figure.

$PEPC_1$, but the effects on these parameters were not very pronounced for $PEPC_2$ (Table II). None of the inhibitors affected V_{max} of either isoform (Table II).

Interacting Effects of Glutamine, DHAP, Glutamate, and 2-Oxoglutarate on $PEPC_1$

In view of the more dramatic responses of $PEPC_1$, the effects of combinations of activators and inhibitors on the isoform were studied in some detail at a fixed subsaturating concentration of PEP. Figure 6A shows that either glutamine or DHAP could relieve the inhibition by glutamate. Equivalent results were obtained when 2-oxoglutarate replaced glutamate as the inhibitor (Fig. 6B). Furthermore, the activating effects of glutamine and DHAP were additive, suggesting separate and independent binding sites for these two effectors.

Native Molecular Mass Estimation

All active fractions ($PEPC_1$ plus $PEPC_2$) from the Q-Sepharose purification step were combined and concentrated to 2 mL by ultrafiltration through a YM-30 membrane. When the concentrate was applied to a Superose 6 gel filtration column, PEPC activity eluted in two peaks. The first peak began to elute at the void volume and was very broad making it impossible to obtain a molecular mass estimate. The second peak corresponded to a molecular mass of 279 ± 21 kD (±SD, n = 3). Experiments where $PEPC_1$ and $PEPC_2$ from the Q-Sepharose step were applied separately to the Superose 6 column showed the $PEPC_1$ corresponded to the low molecular mass form of the enzyme and $PEPC_2$ corresponded to the very high molecular mass form.

DISCUSSION

Effects of NH_4^+ Assimilation on *in Vivo* Activity of PEPC

Resupply of NH_4^+ to N-limited *Selenastrum minutum* cells resulted in an immediate and dramatic (40-fold) increase in the rate of dark carbon fixation (Fig. 1). This was accompanied by a rapid decline in the PEP level and a rapid increase in the malate/PEP ratio (Fig. 2). PEPC activity in crude cell extracts was 30 $\mu mol \cdot mg^{-1}$ Chl $\cdot h^{-1}$ (see "Results"), which was almost sufficient to account for the maximum rate of dark carbon fixation, 40 $\mu mol \cdot mg^{-1}$ Chl $\cdot h^{-1}$ (Fig. 1). This result, coupled with the absence of alternative carboxylating activities, PEP carboxykinase, pyruvate carboxylase, and NAD-malic enzyme (data not shown) indicates that PEPC is the predominant enzyme catalyzing dark carbon fixation in *S. minutum*. This is consistent with ^{13}C isotopic discrimination values observed by Guy *et al.* (5). The decline in PEP, the substrate of PEPC, relative to its produce oxaloacetate (assumed to be in equilibrium with malate) (Fig. 2.) implies that the increased activity of PEPC (dark carbon fixation) during NH_4^+ assimilation is due to activation and not a change in the mass action ratio of this enzyme.

Regulatory Properties of PEPC *in Vitro*

Isolation of Two Isoforms of PEPC

In an attempt to explain the *in vivo* activation of PEPC, the response of this enzyme to various metabolites was studied *in vitro*. This approach was complicated by the fact that two isoforms of PEPC were obtained from *S. minutum* (Table I;

Table III. *Kinetic constants for several effectors of S. minutum $PEPC_1$ and $PEPC_2$*

The standard spectrophotometric assay was used except that the PEP concentration was subsaturating (2.5 mM for $PEPC_1$ and 0.32 mM for $PEPC_2$).

Effector	$PEPC_1$		$PEPC_2$	
	I_{50}	K_a	I_{50}	K_a
		mM		
Glutamine		0.2		ND[a]
DHAP		1.6		ND
Glutamate	3.6		11.6	
2-Oxoglutarate	2.1		4.4	
Aspartate	1.4		9.2	
Malate	3.5		2.9	

[a] Not determined.

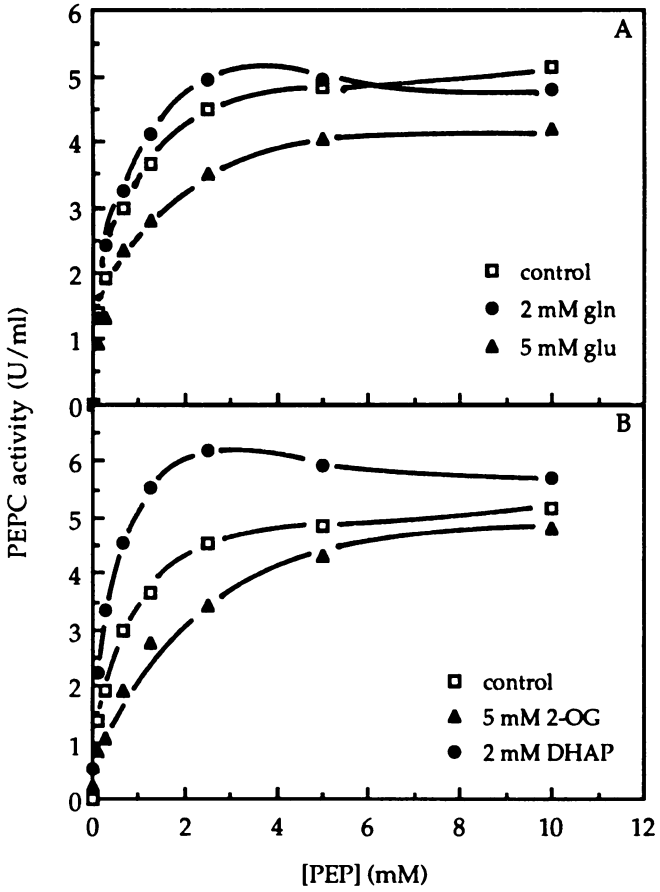

Figure 6. Relationship between $PEPC_1$ activity and the concentration of glutamate (A) and 2-oxoglutarate (B) as determined in the presence and absence of 2 mM DHAP and/or 2 mM glutamine. The standard spectrophotometric assay was used.

Fig. 3). $PEPC_1$ was much more responsive the $PEPC_2$ to most of the regulatory metabolites (glutamine, DHAP, glutamate, 2-oxoglutarate, and aspartate) (Tables II, III; Figs. 4, 5). This could largely by explained by the pronounced sigmoidal PEP saturation kinetics of $PEPC_1$ which contrasted with the typical Michaelis-Menten response of $PEPC_2$ (Figs. 4, 5). $PEPC_1$ had a molecular mass of 279 ± 21 kD as determined by gel filtration chromatography, whereas $PEPC_2$ was a much larger protein eluting as a broad peak beginning at the void volume. $PEPC_1$ and $PEPC_2$ may be distinct isozymes or they may simply be interconvertible forms of the same enzyme. Cytosolic and plastidic isozymes of PEPC have been demonstrated immunologically in two C_3 plants, *Phaseolus* and spinach (26) and interconvertible forms of PEPC are well documented in C_4 and CAM plants (1). However, at present we have no evidence for either of these possibilities in *S. minutum*.

Effect of pH on $PEPC_1$ and $PEPC_2$

The pH profiles of the two forms of *S. minutum* PEPC both showed quite high optima, near pH 9. This might be considered consistent with a plastidic location. However, it is more likely that this high pH optimum is related to the pH stat function of PEPC (12). In other words, as the cytosol becomes more alkaline, PEPC is activated, ultimately resulting in an increase in the malic acid concentration and a return to neutral pH.

Metabolite Effects on $PEPC_1$ and $PEPC_2$

$PEPC_1$ was activated more than 4-fold by 2 mM glutamine and 6-fold by 2 mM DHAP, at a subsaturating PEP concentration of 0.625 mM (Fig. 4). In contrast, $PEPC_2$ showed only 8% activation by glutamine and 52% by DHAP (Fig. 5). Glutamine has been estimated to increase from 0.13 to 25 mM and DHAP from 57 to 330 μM following resupply of NH_4^+ to N-limited *S. minutum* cells (32). Therefore, the glutamine concentration attained *in vivo* is sufficient but the DHAP concentration is somewhat low for maximal activation of PEPC *in vitro* (Table III). The effects of glutamine and DHAP on $PEPC_1$ are additive (Fig. 6B). Consequently, under the conditions given above (2.0 mM glutamine, 2.0 mM DHAP, 0.625 mM PEP), a 10-fold activation of $PEPC_1$ could be expected. This is short of the 40-fold activation seen *in vivo* (Fig. 1) but if declining pool sizes of PEPC inhibitors (32) are also taken into account then we may go further toward explaining the *in vivo* activation of this enzyme.

$PEPC_1$ was more sensitive than $PEPC_2$ to inhibition by glutamate, aspartate, and 2-oxoglutarate but both forms were similarly inhibited by malate (Table III). Preliminary observations indicate that the effects of these inhibitors are not additive (KA Schuller, unpublished data). Glutamate has been estimated to decline from 5.6 to 2.2 mM and 2-oxoglutarate from 0.73 to 0.13 mM following NH_4^+ resupply, but aspartate and malate do not change appreciably over the short term (32). Based on these *in vivo* levels, and the I_{50} values for the various inhibitors (Table III), glutamate and 2-oxoglutarate are likely to be important regulators of *S. minutum* PEPC during enhanced NH_4^+ assimilation. Asparatate and malate may be less important depending on their distribution between and concentration in the various subcellular compartments.

The properties of $PEPC_1$ discussed above and the changes in the pool sizes of the various metabolites (32) are consistent with the rapid increase in the rate of dark carbon fixation following NH_4^+ resupply. However, $PEPC_1$ constituted only 25% of the total activity recovered in the two isoforms of PEPC from *S. minutum* (Table I). Therefore, more detailed studies of the combined effects of the various activators and inhibitors, at PEP and effector concentrations prevailing *in vivo*, are required to determine whether metabolite regulation is sufficient to explain the activation of PEPC during enhanced NH_4^+ assimilation or whether other factors are also involved.

Comparison of S. minutum PEPC with the Enzyme from Other Algae and Higher Plants

Two isoforms of PEPC isolated from the photosynthetic alga *Euglena* were inhibited by malate, citrate, succinate, and 3-phosphoglycerate (25). PEPC purified from leaves of the C_4 plant *Amaranthus viridis* was inhibited by malate, aspartate, 2-oxoglutarate, and glutamate (7). Neither glutamine nor

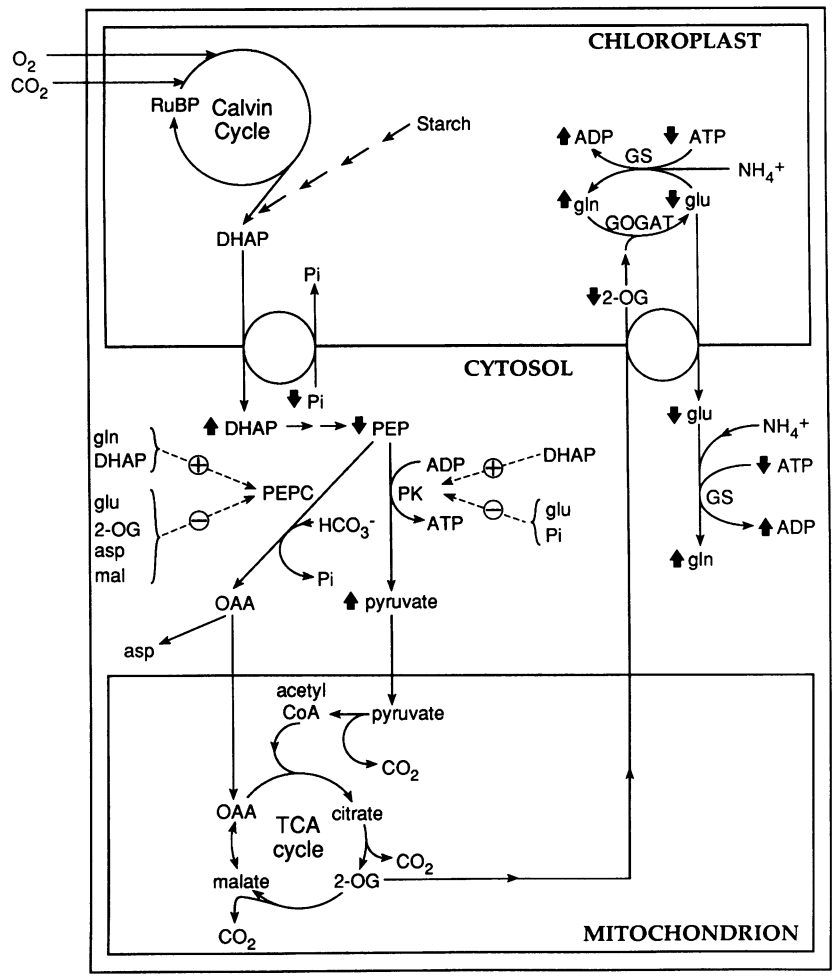

Figure 7. A model for the coordinate regulation of PEPC and PK_c in *S. minutum*. Solid lines represent the flow of metabolites whereas dashed lines indicate regulation of PEPC and PK_c by effectors; (+), activation; (−), inhibition. The broad solid arrows indicate the changes in pool size of the various metabolites following resupply of NH_4^+ to N-limited *S. minutum* cells (30, 32).

DHAP was tested as an effector of either *Euglena* or *Amaranthus* PEPC. PEPC purified to homogeneity from spinach leaves had a K_m(PEP), extrapolated to infinite Mg^{2+}, of 0.1 mM (19). This is the same order of magnitude as the $S_{0.5}$(PEP) of $PEPC_2$ but is very much lower than the $S_{0.5}$(PEP) of $PEPC_1$ (Table II). Also like $PEPC_2$, the PEP saturation curve obtained for the spinach enzyme was hyperbolic (Fig. 5) (19). The native molecular mass of spinach PEPC was 560 kD, which is twice that of $PEPC_1$. None of the metabolites used in the present study were tested as potential effectors of purified spinach PEPC. PEPC from the nodules of a range of legumes is immunologically related to C_4 leaf PEPC (18). This is surprising since it is thought that an important function of PEPC in nodules is anaplerotic carbon fixation (3) as it is in C_3 plant leaves (12). None of the metabolites tested in the present study had any effect on either alfalfa or soybean nodule PEPC where the same compounds were used (27, 33). In contrast, two isoforms of PEPC from lupin nodules were inhibited by aspartate, malate, 2-oxoglutarate, and glutamate (14). Glutamine had no effect.

Coordinate Regulation of PEPC and PK_c during NH_4^+ Assimilation

We have presented evidence that *S. minutum* PEPC is activated in response to an increased requirement for the replenishment of TCA cycle intermediates (particularly 2-oxoglutarate) consumed in the assimilation of NH_4^+ into amino acids. However, if the TCA cycle is to continue to function under the increased demands imposed by NH_4^+ assimilation, then there must be an increased input of acetyl CoA as well as oxaloacetate. In this regard, the cytosolic isozyme of pyruvate kinase (PK_c) from *S. minutum* has been shown to be activated by DHAP and inhibited by glutamate (13), properties shared by PEPC. Since DHAP levels rise and glutamate levels fall following NH_4^+ resupply (30, 32), this would serve to coordinately activate PEPC and PK_c. Activation by DHAP suggests a feed-forward effect due to the activation of glycolysis which has previously been shown to occur following NH_4^+ resupply to N-limited *S. minutum* cells (32). The decline in glutamate can be explained by its rapid conversion to glutamine (catalyzed by glutamine synthetase) in the presence of excess NH_4^+.

The unique feature of PEPC is its activation by glutamine. As glutamate and 2-oxoglutarate levels fall following NH_4^+ resupply, glutamine levels rise (30, 32). The rise in glutamine can be explained by a limitation on GOGAT activity imposed by the falling 2-oxoglutarate level. Rising glutamine and falling 2-oxoglutarate would serve to activate PEPC, resulting in replenishment of TCA cycle intermediates and consequent alleviation of any 2-oxoglutarate limitation on GOGAT activity. Conversely, when NH_4^+ assimilation ceases, due to NH_4^+

depletion, glutamine levels would be expected to fall and glutamate levels to rise, thereby inhibiting PEPC. In this way, PEPC activity may be linked to carbon skeleton (2-oxoglutarate) availability for NH_4^+ assimilation. Figure 7 summarizes the regulatory properties of PK_c and PEPC and integrates them into a model of the anaplerotic function of PEPC during NH_4^+ assimilation.

ACKNOWLEDGMENTS

We are grateful to H. Hansford for maintaining chemostat cultures; R. Feil, A. Chadderton, and K. Vlossak for physiological data; and G. C. Vanlerberghe and Drs. F. C. Botha and R. G. Smith for enlightening discussions.

LITERATURE CITED

1. **Andreo CS, Gonzalez DH, Iglesias AA** (1987) Higher plant phosphoenolpyruvate carboxylase: structure and regulation. FEBS Lett **213:** 1–8
2. **Bradford MM** (1976) A rapid sensitive method for quantitation of microgram quantities of protein utilizing the principle of protein-dye binding. Anal Biochem **72:** 248–253
3. **Deroche M-E, Carrayol E** (1988) Nodule phosphoenolpyruvate carboxylase: a review. Physiol Plant **74:** 775–782
4. **Elrifi IR, Turpin DH** (1986) Nitrate and ammonium induced photosynthetic suppression in N-limited *Selenastrum minutum*. Plant Physiol **81:** 273–279
5. **Guy RD, Vanlerberghe GC, Turpin DH** (1989) Significance of phosphoenolpyruvate carboxylase during ammonium assimilation: carbon isotope discrimination in photosynthesis and respiration by the N-limited green alga *Selenastrum minutum*. Plant Physiol **89:** 1150–1157
6. **Hammel KE, Cornwell KL, Bassham JA** (1979) Stimulation of dark CO_2 fixation in isolated mesophyll cells of *Papaver sonniferum* L. Plant Cell Physiol **20:** 1523–1529
7. **Iglesias AA, Gonzalez DH, Andreo CS** (1986) Purification and molecular and kinetic properties of phosphoenolpyruvate carboxylase from *Amaranthus viridis* L. leaves. Planta **168:** 239–244
8. **Jiao J, Chollet R** (1988) Light/dark regulation of maize leaf phosphoenolpyruvate carboxylase by *in vivo* phosphorylation. Arch Biochem Biophys **261:** 409–417
9. **Job D, Cochet C, Dhien A, Chambaz E** (1978) A rapid method for screening inhibitor effects: determination of I_{50} and its standard deviation. Anal Biochem **84:** 68–77
10. **Kanazawa T, Kirk MR, Bassham JA** (1970) Regulatory effects of ammonia on carbon metabolism in photosynthesizing *Chorella pyrenoidosa*. Biochem Biophys Acta **205:** 401–408
11. **Larsen PO, Cornwell KL, Gee SL, Bassham JA** (1981) Amino acid synthesis in photosynthesizing spinach cells: effects of ammonia on pool sizes and rate of labeling from $^{14}CO_2$. Plant Physiol **68:** 292–299
12. **Latzko E, Kelly GJ** (1983) The many-faceted function of phosphoenolpyruvate carboxylase in C_3 plants. Physiol Veg **21:** 805–815
13. **Lin M, Turpin DH, Plaxton WC** (1989) Pyruvate kinase isozymes from the green alga, *Selenastrum minutum*. II. Kinetic and regulatory properties. Arch Biochem Biophys **268:** 228–238
14. **Marczewski W** (1989) Kinetic properties of phosphoenolpyruvate carboxylase from lupin nodules and roots. Physiol Plant **76:** 539–543
15. **McNaughton GAL, Fewson CA, Wilkins MB, Nimmo HG** (1989) Purification, oligomerization state and malate sensitivity of maize leaf phosphoenolpyruvate carboxylase. Biochem J **261:** 349–355
16. **Melzer E, O'Leary M** (1987) Anaplerotic CO_2 fixation by phosphoenolpyrivate carboxylase in C_3 plants. Plant Physiol **84:** 58–60
17. **Miflin BJ, Lea PJ** (1982) Ammonia assimilation and amino acid metabolism. *In* D Boulton, B Parthier, eds, Encyclopedia of Plant Physiology (New Series), Vol 14A. Springer-Verlag, New York, pp 5–64
18. **Miller SS, Boylan KLM, Vance CP** (1987) Alfafa root nodule carbon dioxide fixation. III. Immunological studies of nodule phosphoenolpyruvate carboxylase. Plant Physiol **18:** 501–508
19. **Miziorko HN, Nowak T, Mildvan AS** (1974) Spinach leaf phosphoenolpyruvate carboxylase: purification, properties and kinetic studies. Arch Biochem Biophys **168:** 378–389
20. **Nimmo GA, Nimmo HG, Hamilton ID, Fewson CA, Wilkins MB** (1986) Purification of the phosphorylated night form and dephosphorylated day form of phosphoenolpyruvate carboxylase from *Bryophyllum fedtschenkoi*. Biochem J **239:** 213–220
21. **Ohmori M** (1981) Effect of ammonia on dark CO_2 fixation of *Anabaena* cells treated with methionine sulfoximine. Plant Cell Physiol **22:** 709–716
22. **Ohmori M, Wolf FR, Bassham JA** (1984) *Botryococcus braunii* carbons/nitrogen metabolism as affected by ammonia addition. Arch Microbiol **140:** 101–106
23. **O'Leary MH** (1982) Phosphoenolpyruvate carboxylase: an enzymologist's view. Annu Rev Plant Physiol **33:** 297–315
24. **Paul JS, Cornwell KL, Bassham JA** (1978) Effects of ammonia on carbon metabolism in photosynthesizing isolated mesophyll cells from *Papaver sonniferum* L. Planta **142:** 49–54
25. **Peak JG, Peak MJ** (1981) Heterotrophic carbon fixation by *Euglena*: function of phosphoenolpyruvate carboxylase. Biochim Biophys Acta **677:** 390–396
26. **Perrot-Rechenmann C, Vidal J, Brulfert J, Burlet A, Gadal P** (1982) A comparative immunocytochemical localization study of phosphoenolpyruvate carboxylase in leaves of higher plants. Planta **55:** 24–30
27. **Peterson JB, Evans HJ** (1979) Phophoenolpyruvate carboxylase from soybean nodule cytosol: evidence for isozymes and kinetics of the most active component. Biochim Biophys Acta **567:** 445–452
28. **Podesta FE, Andreo CS** (1989) Maize leaf phosphoenolpyruvate carboxylase: oligomeric state and activity in the presence of glycerol. Plant Physiol **90:** 427–433
29. **Selinioti E, Nikolopoulos D, Manetas Y** (1987) Organic cosolutes as stabilisers of phosphoenolpyruvate carboxylase in storage: an interpretation of their action. Aust J Plant Physiol **14:** 203–210
30. **Smith RG, Vanlerberghe GC, Stitt M, Turpin DH** (1989) Short-term metabolite changes during transient ammonium assimilation by the N-limited green alga *Selenastrum minutum*. Plant Physiol **91:** 749–755
31. **Stamatakis K, Gavalas NA, Manetas Y** (1988) Organic cosolutes increase the catalytic efficiency of phosphoenolpyruvate carboxylase, from *Cynodon dactylon* (L.) Pers., apparently through self-association of the enzymic protein. Aust J Plant Physiol **15:** 621–631
32. **Turpin DH, Botha FC, Smith RG, Feil R, Horsey AK, Vanlerberghe GC** (1990) Regulation of carbon partitioning to respiration during dark ammonium assimilation in the green alga *Selenastrum minutum*. Plant Physiol **93:** 166–175
33. **Vance CP, Stade S** (1984) Alfafa root nodule carbon dioxide fixation. II. Partial purification and characterization of root nodule phosphoenolpyruvate carboxylase. Plant Physiol **75:** 261–264
34. **Vanlerberghe GC, Horsey AK, Weger HG, Turpin DH** (1989) Anaerobic carbon metabolism by the TCA cycle: evidence for partial oxidative and reductive pathways during dark ammonium assimilation. Plant Physiol **91:** 1551–1557
35. **Wu M-X, Wedding RT** (1985) Regulation of phosphoenolpyruvate carboxylase from *Crassula* by interconversion of oligomeric forms. Arch Biochem Biophys **240:** 655–662
36. **Wu M-X, Wedding RT** (1987) Regulation of phosphoenolpyruvate carboxylase from *Crassula argentea*: further evidence on the dimer-tetramer interconversion. Plant Physiol **84:** 1080–1083